

# Langendorff Heart: A Model System To Study Cardiovascular Effects of Engineered Nanoparticles

Andreas Stampfl,<sup>†,\*</sup> Melanie Maier,<sup>†</sup> Roman Radykewicz,<sup>†</sup> Peter Reitmeir,<sup>‡</sup> Martin Göttlicher,<sup>†</sup> and Reinhard Niessner<sup>§</sup>

<sup>†</sup>Institute of Toxicology and <sup>‡</sup>Institute of Health Economics & Healthcare Management, Helmholtz Zentrum München, German Research Center for Environmental Health, Ingolstädter Landstrasse 1, D-85764 Neuherberg, Germany, and <sup>§</sup>Chair of Analytical Chemistry, Technische Universität München, Marchioninistrasse, 17, D-81377 München, Germany

Development and production of engineered nanoparticles (ENPs) are an emerging technology for use in various technical and medical applications, for example, as transporters for drugs in the human body. For example they are used as gene carriers to tumors in a concentration of 50  $\mu\text{g}$  per 20 g body weight.<sup>1</sup> This applied concentration corresponds to 37  $\mu\text{g}/\text{mL}$  blood for a human with 75 kg of body weight and 5 L of blood volume. Compared to our experiments the highest used P90 concentration of  $8 \times 10^9$  particles/mL corresponds to a weight of approximately 6  $\mu\text{g}/\text{mL}$  and the highest concentration of  $\text{TiO}_2$  ( $4 \times 10^9$  particles/mL) corresponds to 9  $\mu\text{g}/\text{mL}$ . However, the effects on the organism in total are largely unknown and often seen as a possible risk. From epidemiological studies it has been long known that nanoparticles in ambient air exert negative effects on the cardiovascular system and central nervous system (CNS).<sup>2–7</sup> It is conceivable that newly developed ENPs may also have a negative impact on the cardiovascular system upon exposure. Investigations using inhalation and instillation of nanoparticles unambiguously showed their respiratory toxicity and inflammation reactions.<sup>8</sup>

On the cellular level different tests are routinely used. These tests possess different end points and elucidate only one parameter. Hence, they cannot accurately predict an *in vivo* response, necessarily. However, up to this point, toxicity tests on internal organs with respect to ENPs have not been described, but the establishment of such is highly requested.<sup>9–11</sup>

Three-dimensional test systems can be used to assess part of the risk potential of the ENPs. With these models complex body barrier structures are simulated *in vitro* and the translocation of ENPs can be studied. For example, human skin and air tubing can be

**ABSTRACT** Engineered nanoparticles (ENPs) are produced and used in increasing quantities for industrial products, food, and drugs. The fate of ENPs after usage and impact on health is less known. Especially as air pollution, suspended nanoparticles have raised some attention, causing diseases of the lung and cardiovascular system. Human health risks may arise from inhalation of ENPs with associated inflammation, dispersion in the body, and exposure of vulnerable organs (e.g., heart, brain) and tissues with associated toxicity. However, underlying mechanisms are largely unknown. Furthermore future use of ENPs in therapeutic applications is being researched. Therefore knowledge about potential cardiovascular risks due to exposure to ENPs is highly demanded, but there are no established biological testing models yet. Therefore, we established the isolated beating heart (Langendorff heart) as a model system to study cardiovascular effects of ENPs. This model enables observation and analysis of electrophysiological parameters over a minimal time period of 4 h without influence by systemic effects and allows the determination of stimulated release of substances under influence of ENPs. We found a significant dose and material dependent increase in heart rate accompanied by arrhythmia evoked by ENPs made of flame soot (Printex 90), spark discharge generated soot, anatase ( $\text{TiO}_2$ ), and silicon dioxide ( $\text{SiO}_2$ ). However, flame derived  $\text{SiO}_2$  (Aerosil) and monodisperse polystyrene lattices exhibited no effects. The increase in heart rate is assigned to catecholamine release from adrenergic nerve endings within the heart. We propose the isolated Langendorff heart and its electrophysiological characterization as a suitable test model for studying cardiovascular ENP toxicity.

**KEYWORDS:** Langendorff heart · engineered nanoparticles · catecholamines · ECG · nanotoxicity

built up as three-dimensional *in vitro* test systems and offer the possibility to check any impact of ENPs.<sup>12</sup>

The mechanisms involved for cardiovascular effects of nanoparticles are poorly understood, in general. So far, only the method of translocation of deposited nanoparticles from the lung, through lung tissue or membrane, to the bloodstream, and consequently to other organs has been published previously.<sup>13,14</sup> Therefore, it would be very valuable to have a model system to test the impact on the heart as an intact organ. It is currently unclear, whether NPs (and consequently also ENPs) can affect the cardiovascular system

\* Address correspondence to stampfl@helmholtz-muenchen.de.

Received for review September 23, 2010 and accepted June 1, 2011.

Published online June 01, 2011  
10.1021/nn200801c

© 2011 American Chemical Society

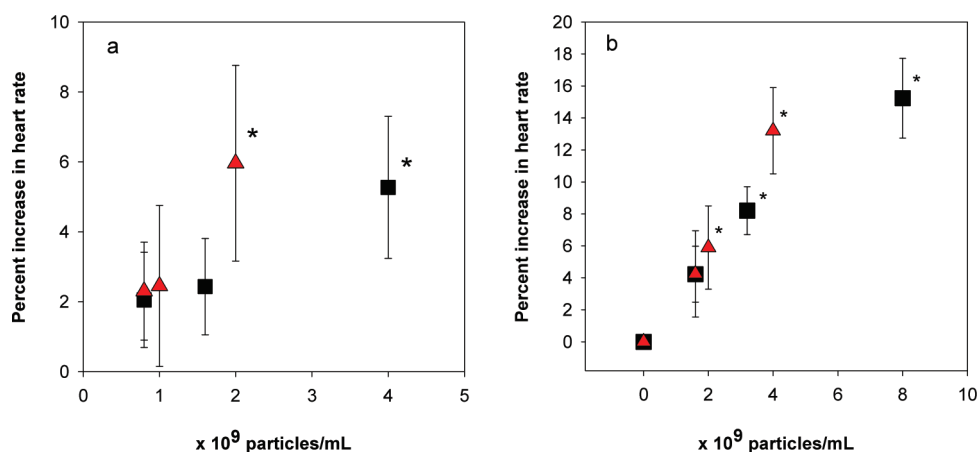


**Figure 1.** Dose-dependent increase in heart rate compared to baseline (nearby 180 BPM) before exposure (mean value  $\pm$  SD;  $n = 6$  each; \*,  $p < 0.05$ ): (a) 1 h after ENPs exposure, (b) 2 h after ENPs exposure (after 1 h particle concentration was doubled). TiO<sub>2</sub>, red triangle; P90, black square.

by causing systemic inflammation, stimulating metabolic effects, or whether they can act directly (physically) on the heart.

We report on our experiments with an isolated beating heart, the so-called Langendorff heart (LH).<sup>15–18</sup> It has its own rhythm generator, the sinus node, and is still beating outside the organism. Guinea pigs were chosen as donor animals, as their electrophysiological response in the ECG is similar to that of humans. Other rodents have only a very short ST segment, so that alterations, such as ST elevations, can hardly be detected. We modified the well established LH system for isolated hearts and adapted a second volume for recirculation of the perfusion solution after a washout period. The ENP solution was added to the same vessel.

The function of the heart is monitored by the ECG and by determination of the perfusion rate. The LH allows the perfusion with different kinds of fluid-dispersed particles, and, of special importance, the reversibility of the observed effect by repetitive rinsing of the heart with particle-free buffer can be studied. Furthermore, chemical analysis of the perfusion solution allows for interpretation, whether the observed effects are directly evoked by ENPs or neuronal, hormonal, or inflammatory effects are involved.

This provides an adequate model for testing the effects of ENPs on the heart rate measured by ECG. It also offers the chance for analysis of possible released catecholamines stemming from nerve endings within the heart and other originated substances during ENP perfusion. First experiments have shown that particles can affect ECG, heart rate, and catecholamine release in this model.<sup>19</sup>

## RESULTS

We added different defined amounts of appropriate model ENP materials to the recirculating perfusion solution of the isolated hearts after an initial equilibration period. Typically, the heart rate before adding the particles was approximately 180 beats per minute (BPM). During

the first hour after addition of ENP, a significant dose-dependent increase in heart rate occurred, and a steady state level was reached. TiO<sub>2</sub> ( $2 \times 10^9$  particles/mL) increased the heart rate significantly by  $5.96 \pm 2.8\%$  and Printex 90 ( $4 \times 10^9$  particles/mL) by  $5.27 \pm 2.03\%$  (Figure 1a). To elucidate, whether the particles have more effectiveness after a first contact, the concentration after the first hour was doubled. After doubling, a further increase in heart rate occurred which was accompanied by cardiac arrhythmia. The increase was stronger than after the initial dose. Two hours after application of nanoparticulate TiO<sub>2</sub> ( $4 \times 10^9$  particles/mL) the heart rate increased significantly by  $13.2 \pm 2.7\%$  ( $n = 7$ ;  $p < 0.05$ ), and under the influence of flame soot P90 ( $8 \times 10^9$  particles/mL) the heart rate increased by  $15.2 \pm 2.5\%$  ( $n = 7$ ;  $p < 0.05$ ) (see Figure 1b) as well.

Furthermore, we investigated the effect of SiO<sub>2</sub> and spark discharge generated soot without dose-dependency at one concentration level each. One hour after application spark discharge generated soot evoked a significant increase in heart rate. After doubling the concentration the heart frequency increased significantly during the second hour under the influence of spark discharge generated soot, and SiO<sub>2</sub> as well. Moreover, arrhythmia also occurred. SiO<sub>2</sub> was the most efficacious material. In a concentration of  $1 \times 10^9$  particles/mL the increase in heart rate was 7% at the end of the second hour. Spark discharge generated soot ( $8 \times 10^9$  particles/mL) evoked an increase by 13% during the second hour (Figure 2). The particle size was controlled during the entire experiment to exclude agglomeration.

In the absence of particles, the heart rate did not change for 3 h, and no significant alterations in the ECG were observed (data not shown).

To summarize the effects of flame soot P90, TiO<sub>2</sub>, and spark discharge generated soot, the same concentration and same duration of exposure is shown in Figure 3 with a typical experiment each.

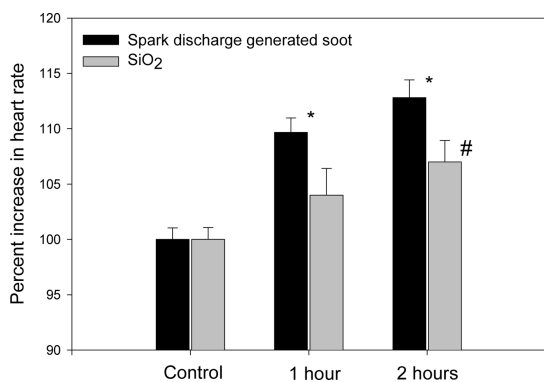


**Figure 2.** Increase in heart rate evoked by spark discharge generated soot and SiO<sub>2</sub>. Increase in heart rate after 1 h spark discharge generated soot exposure ( $4 \times 10^9$  particles/mL) and 2 h after doubling of the particle concentration ( $8 \times 10^9$  particles/mL); (mean value  $\pm$  SD;  $n = 6$  each; \*, #:  $p < 0.05$ ). Increase in heart rate after 1 h SiO<sub>2</sub> exposure ( $5 \times 10^9$  particles/mL) and 2 h after doubling of the particle concentration ( $1 \times 10^9$  particles/mL); (mean value  $\pm$  SD;  $n = 6$  each; \*, #:  $p < 0.05$ ).

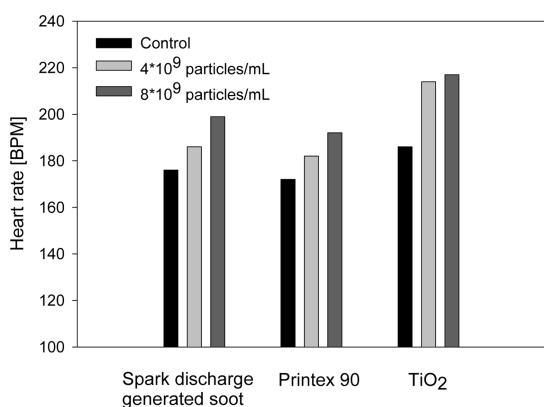


**Figure 3.** Increase in heart rate after 1 h ( $4 \times 10^9$  particles/mL) and 2 h after doubling of the particle concentration ( $8 \times 10^9$  particles/mL) of exposure with TiO<sub>2</sub>, P90, and spark discharge generated soot. One typical experiment for each material is shown.

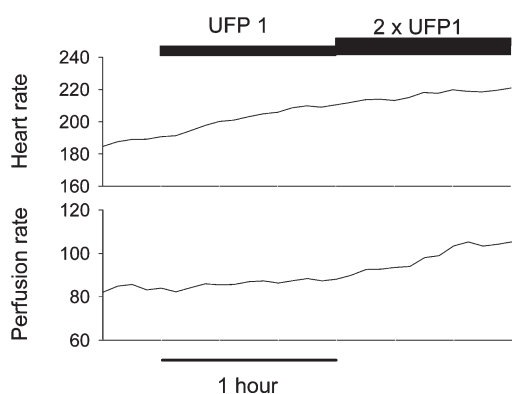


**Figure 4.** Time-resolved correlation between heart frequency and coronary flow during exposure of TiO<sub>2</sub> ( $2 \times 10^9$  and  $4 \times 10^9$  particles/mL) for one single experiment.

Concomitantly to the increase in heart rate, an increase in coronary flow through the heart was observed (Figure 4). The increase in perfusion rate is a hint

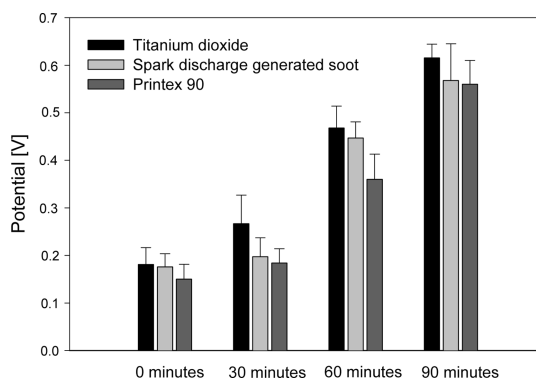


**Figure 5.** ST elevation after particle application of TiO<sub>2</sub>, spark discharge generated soot, and P90 ( $n = 3$ ).

that the bloodstream is not reduced by occlusion of vessels.

Simultaneously with the heart rate, the ECG was altered under the influence of these particles. After particle application ST elevations occurred (see Figure 5). Atrio-ventricular block (AV block) appeared at the highest used concentrations of P90 at  $44 \pm 4$  min, TiO<sub>2</sub> at  $50 \pm 5$  min, and spark discharge generated soot at  $27 \pm 3$  min after addition of the particles ( $n = 3$ ). Typical ECGs are shown in Figure 6. An AV block involves the impairment of the conduction between the atria and ventricles of the heart. The increased coronary flow corresponding to the increase in heart rate indicated that the observed changes in ECG, especially ST elevations, were actually induced by particles and not evoked by ischemia.

During the following washout period of 30 min, the heart rate returned to the initial value. The ECG changes (ST elevations and AV blocks) however, persisted.

Regarding the observed decrease in heart rate during the washout period with particle-free perfusion solution, we hypothesized that the ENP-induced increase in heart rate might be caused by a release of catecholamines from the sympathetic nerve endings in the heart.

To examine this hypothesis, in a first approach, we blocked the catecholamine  $\beta_1$ -receptors using metoprolol ( $3 \mu\text{g/mL}$ ). When this inhibitor was added after the first hour of the perfusion period with the ENP suspension, the heart rate decreased rapidly within a few minutes by  $13.7 \pm 2.2\%$  ( $n = 6$ ). This effect was observed with flame soot P90 and TiO<sub>2</sub>. When metoprolol was administered before adding the ENPs, no effect was observed because the catecholamine receptors were blocked before the ENPs evoked a release of catecholamines.

In a second experiment, we pretreated guinea pigs before heart excision with reserpine (subcutaneous injection of 5 mg/kg bodyweight) for 24 h. This application effectively depletes catecholamine stores in neurons.<sup>20,21</sup> Under these conditions, TiO<sub>2</sub> ( $4 \times 10^9$  particles/mL) failed to increase the heart rate in the isolated hearts.

To get direct evidence that catecholamines evoke the increase in heart rate, in some experiments aliquots of the perfusion solution were collected before and 2 h

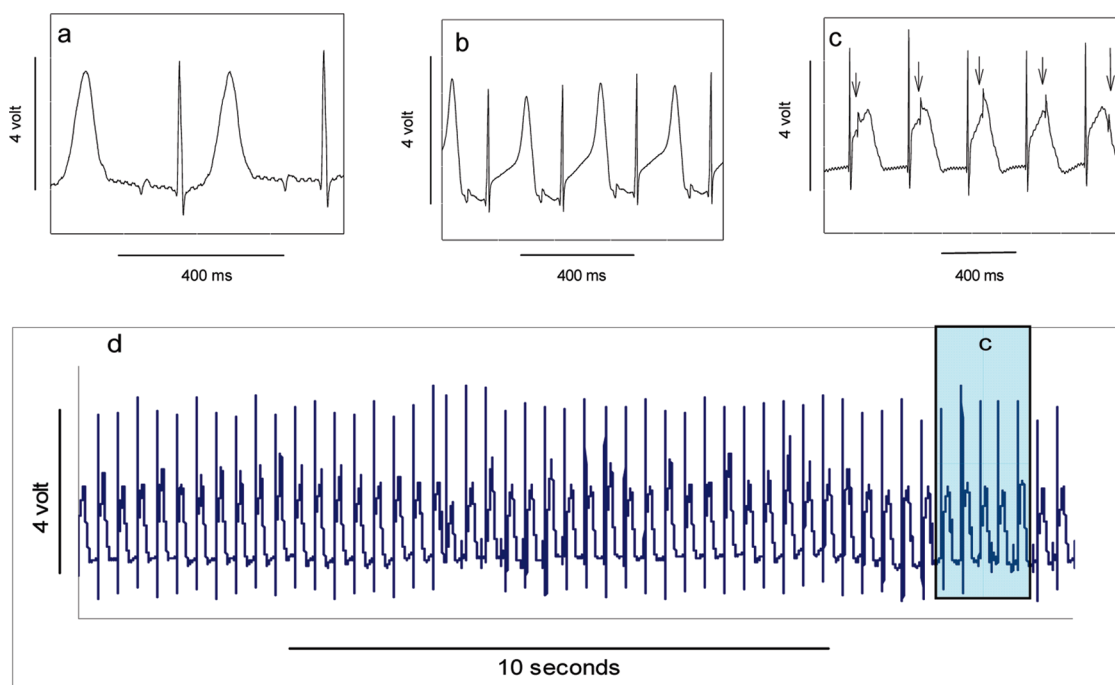


**Figure 6.** ECG graphs show ST elevation and AV block after ENPs instillation: (a) control; (b) ST elevation; (c) AV block; (d) AV block in a prolonged period (extended part from Figure 6c). Typical ECGs are shown.

after adding ENPs, and the total catecholamine content was determined by HPLC analysis. Primarily, noradrenalin (NA) was detected. At concentrations of flame soot P90 and  $\text{TiO}_2$ , that exhibited similar effects on the heart rate, the NA content was significantly elevated by 69% ( $n = 7$ ;  $p < 0.002$ ) compared to the level observed before addition of NP. In two control experiments without ENP addition, no increase in NA content was detected. However with the ENP samples, made of Aerosil 90, 200, 380, and polystyrene lattices no alterations in heart frequency and ECG were observed. Moreover, in three experiments with Aerosil 200 the NA content was determined, and no increase after application of the drug was observed, too.

For further understanding of the release mechanism of catecholamines we proved whether calcium ions play a key role. Therefore, we determined the intracellular free calcium in single neurons by fluorescence imaging using the  $\text{Ca}^{2+}$ -sensitive fluorescent dye Fura-2. In mouse neuroblastoma cells (Neuro2A) flame soot P90 and  $\text{TiO}_2$  evoked a significant increase in intracellular free calcium within 30 min.  $\text{TiO}_2$ , in a concentration of  $4 \times 10^9$  particles/mL, was similarly provocative as flame soot P90 in a concentration of  $8 \times 10^9$  particles/mL (Figure 7). This finding corresponds to the effects of these particles on the increase in heart rate.

## DISCUSSION

Our results show that ENPs directly affect the heart function of the LH model. The observed increase in heart rate is very likely caused by a release of catecholamines from the neural endings at the inner heart

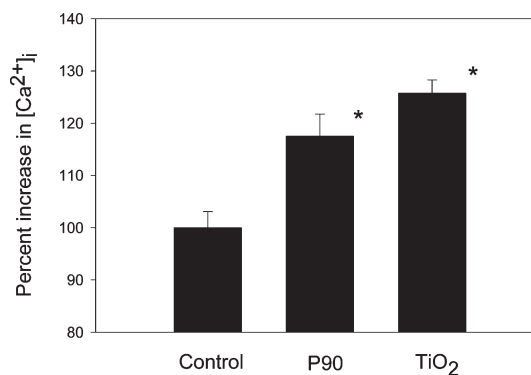


**Figure 7.** Increase in intracellular free calcium ( $[\text{Ca}^{2+}]_i$ ) evoked by P90 and  $\text{TiO}_2$ . Increase in intracellular free calcium in Neuro2A cells 30 min after the addition of P90 and  $\text{TiO}_2$  (mean value  $\pm$  SE;  $n \geq 13$ ; \*,  $p < 0.001$ ).

walls after particle/cell wall interaction. However, it cannot be totally ruled out that catecholamine reuptake is diminished by inhibition of their specific transporters. Some control experiments with the reuptake inhibitor reboxetine had no influence on heart rate.

Another study using isolated hearts of hypertensive rats also found a slight increase in heart rate after application of 50 and 100  $\mu\text{g/mL}$  suspended dust particles.<sup>17</sup> In our experiments with guinea pig hearts, we found a significant increase by about 15% after application of only  $8 \times 10^9$  particles/mL flame soot P90, corresponding to about 6  $\mu\text{g/mL}$ . This difference of about 1 order of magnitude may be due to the different materials and different animal species used. In any case, the prevalent mechanisms appear to be functional on the axons or nerve endings per se, since

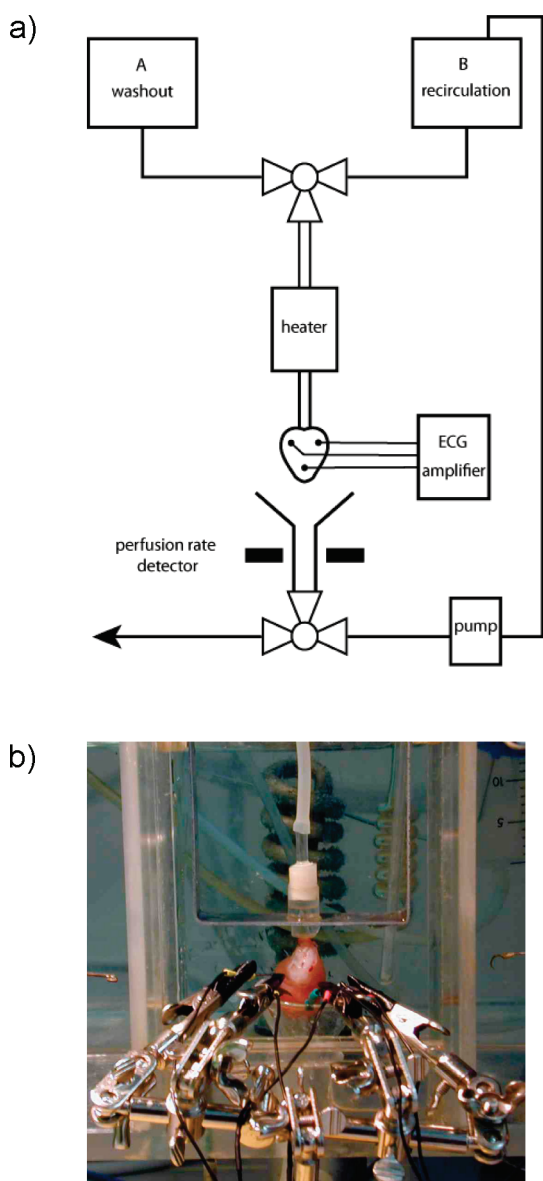


Figure 8. The Langendorff heart apparatus.

in the LH the adrenergic nerve endings are separated from the nerve cell bodies in the spinal ganglia.

This assumption could also be encouraged by the observation that diesel exhaust particles evoke significant ECG changes in guinea pig hearts, that is, AV block.<sup>22</sup> In the brain, the same type of particles also induced changes in EEG of human volunteers.<sup>23</sup> Moreover, it has been shown that ultrafine carbon black particles can affect the ECG and heart rate in young healthy humans.<sup>24</sup>

In the case of AV block increased vagal tone would be an alternative consideration, whereas increased junctional automaticity and interference dissociation is in line with our hypothesis that catecholamines are released.

It seems therefore quite reasonable to look for a means to prove any influence of ENPs onto the heart function. As we can see from the above-described results, the LH model seems to have potential to serve as a test

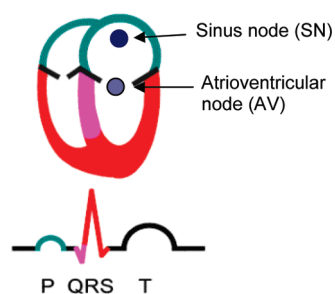


Figure 9. Scheme of an ECG corresponding to the heart parts.

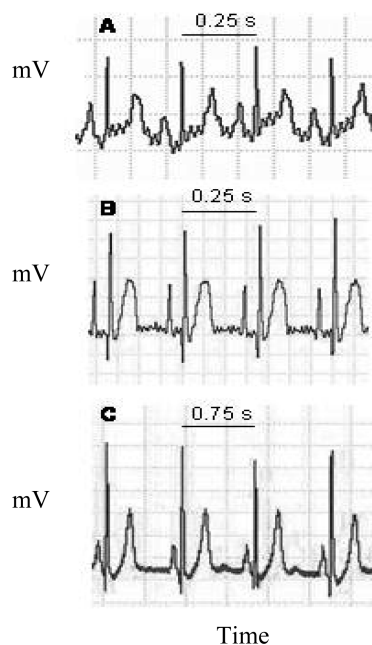


Figure 10. (A) ECG of the guinea pig, (B) ECG of the isolated heart from the same animal; (C) ECG of a human. Note: Panel C shows a different time scale.

TABLE 1. Differences between Human and Guinea Pig ECG Parameters

ECG parameter	human	guinea pig
heart rate	80 beats/min	240 beats/min
P wave	0.05–0.1 s	≤0.02 s
PR interval	0.13–0.2 s	≤0.07 s
QT interval	0.18–0.52 s	≤0.14 s
QRS duration	0.05–0.1 s	≤0.03 s

system. The observed effects can be explained in different ways. In the simplest manner the particles affect the neurons and cause them to release noradrenaline. Second, it may be possible that ENPs evoke a release of endothelin from endothelial cells in the heart, which enhances the release of noradrenaline from the nerve endings. Endothelin plays an important role in the central and peripheral sympathetic nervous system. It can stimulate an increased release of catecholamine. It has been shown that endothelin acts directly at chromaffin cells existing in the sympathetic nerve and leads to an increase

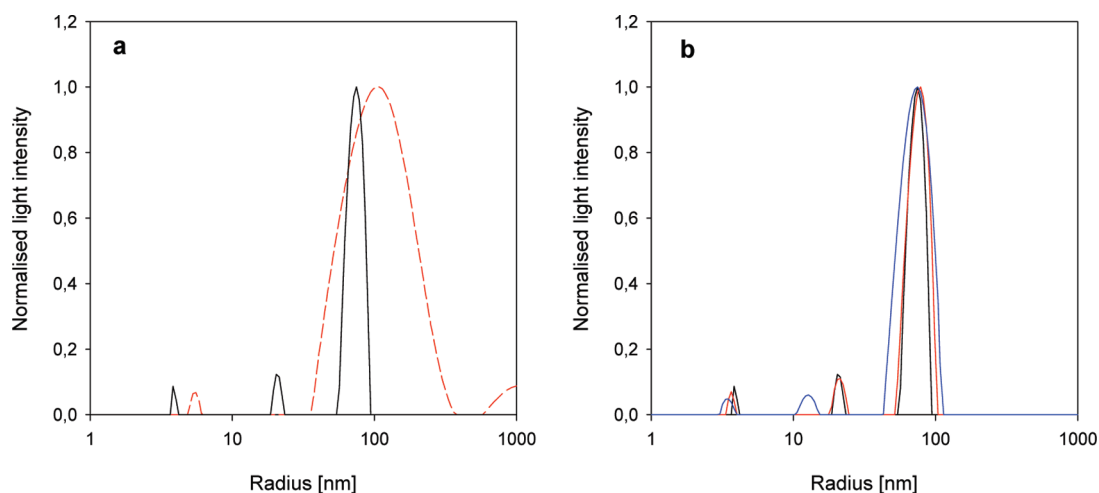


Figure 11. Particle size distribution. (a) Comparison of unfiltered (red dashed line) and filtered (black solid line) P90 stock suspensions. (b) Stock solution after filtration (control; black line), after 2 h (red line), and after 6 h (blue line).

TABLE 2. Applied Engineered Nanoparticles

partide type	chemical composition	specific surface area	manufacturer	diameter (nm)	production process
Aerosil 90	SiO <sub>2</sub>	90	Degussa, Hanau, Germany	20	continuous flame hydrolysis
Aerosil 200	SiO <sub>2</sub>	200	Degussa, Hanau, Germany	12	continuous flame hydrolysis
Aerosil 380	SiO <sub>2</sub>	380	Degussa, Hanau, Germany	7	continuous flame hydrolysis
titanium dioxide (anatase)	TiO <sub>2</sub>	50	Degussa, Hanau, Germany	20	continuous flame hydrolysis
Printex 90	carbon	272	Degussa, Hanau, Germany	14	flame derived soot
lattices	polystyrene	70	Duke Scientific Corporation, Palo Alto, California	41	emulsion polymerization
spark discharge generated soot	carbon	395	GFG 1000 Palas, Karlsruhe, Germany	120	spark discharge across graphite electrodes
silicon dioxide	SiO <sub>2</sub>	400	Sigma Aldrich, Steinheim, Germany	7	continuous flame hydrolysis

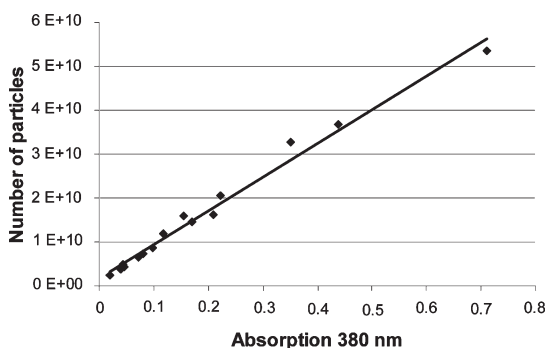


Figure 12. Particle concentration of Printex 90 versus measured absorption. Linear regression line:  $y = 8 \times 10^{10} \times x$ ;  $R^2 = 0.9797$ ;  $n = 6$ .

in intracellular calcium, which in turn results in catecholamine release.<sup>25</sup> It is shown, that Endothelin-1 receptors exist in the sympathetic nerve varicosities in guinea pig heart.<sup>26</sup>

A further possible mechanism underlying the effect of ENPs on neurons might be the production of reactive oxygen species (ROS). It has been shown repeatedly that ultrafine particulate pollutants induce oxidative stress and mitochondrial and DNA damage.<sup>27–33</sup>

Since endothelial cells can be a target and a source for ROS, interaction between ROS and the endothelium seems to play an important role in cardiovascular homeostasis.<sup>34–36</sup>

On the one hand, ROS can directly affect neurons to release noradrenaline, and on the other hand ROS can induce release of endothelin,<sup>37</sup> both leading to an increase in heart rate. The endothelial dysfunction is another indication for the impact of ENPs on the cardiovascular system. Studies on a possible interaction of stimulated ROS are currently being performed but are beyond scope of this contribution.

## CONCLUSION

We present the LH as a very promising model to test the toxicity of ENPs on the heart. Our study provides experimental evidence that certain nanoengineered materials modulate the rhythm of the isolated heart. We demonstrated for the first time that ENPs can exert direct effects on the heart. These findings support observations from epidemiological studies that nanoparticle exposure may affect heart rhythm, heart rate variability,<sup>38</sup> and cardiac morbidity. The effects of ENPs on the heart are probably mediated by alterations of catecholamine turnover and give rise to the assumption that ENPs could also adversely affect other neuronal functions of the autonomic nervous system.<sup>39,40</sup> Our findings on the impact of distinct ENPs on calcium homeostasis in neurons are a fundamental hint for this. Other fluoroprobes could be also used to measure biochemical changes such as pH, oxidative stress,

and membrane potential. Using thin glass fibers, fluorescence measurements within the heart would be feasible.

In contrast to TiO<sub>2</sub>, P90, SiO<sub>2</sub>, and spark discharge generated soot particles; those consisting of flame-derived SiO<sub>2</sub> (Aerosil) and PSL particles had no influence on heart rate and evoked no arrhythmia. These differences may depend on different unknown surface properties (e.g., hydrophilicity). Aerosil and polystyrene particles are perfectly round-shaped and of high hydrophobicity.<sup>41</sup>

Thus, the LH model system is a suitable method to test new nanomaterials for possible negative impacts on the cardiac system and to understand their mechanisms of action. Additional information on the cardiac function

and heart wall motion could be obtained from 3D ultrasonic tomography. This would allow a continuous measurement during the cardiac cycle and could detect local disturbances. In the recirculated perfusion liquid different substances that are released from the heart can be determined. Furthermore, the LH enables the possibility to get information about the influence of ENPs on neurons by analyzing the heart rate.

In conclusion, the LH system is attractive due to easy handling, sensitivity, and instantaneous response. Findings correlate well with epidemiological knowledge from air hygiene studies and may be transferable to humans. Finally, the heart tissue can be used for further investigations of gene expression or proteomic studies evoked by ENPs.

## METHODS

**Langendorff Heart (LH).** The LH is an isolated heart, which is retrograde perfused via the coronary arteries, and allows one to study cardiac activity. As a basic principle, two types of LH are known: the constant pressure and the constant flow LH. For our experiments we applied Langendorff heart equipment under constant pressure conditions, using the hydrostatic pressure between the vessels and the heart, thus simulating the blood pressure. The constant flow system may have the disadvantage that under reduced flow conditions, evoked by NP, the pressure will increase in order to keep the flow constant. When the perfusion pressure becomes too high, cardiac tissue edema may develop. In contrast to the well-known system, we therefore extended the test system by a second vessel (see Figure 8a).

The buffer in vessel A (Figure 8a) is used to wash out the blood from the heart. The level in vessel A is kept constant using an optical filling sensor, guiding the refilling pump. After a wash out period the heart is perfused with buffer from vessel B. After passing through the heart, this buffer is recirculated to vessel B. The advantage of the recirculation is that experiments lasting a long time require only a small amount of the selected particle material. Moreover, the great advantage is the possibility to obtain samples for further analysis of substances which were released from the heart under the influence of ENPs. Furthermore, the solution in the vessels was saturated with oxygen, and the system temperature was kept constant to 37.5 °C.

**Animals and Heart Preparation.** Wild type guinea pigs of both sexes (250–350 g body weight) were purchased from Charles River WIGA GmbH (D-97633 Sulzfeld, Germany). All experiments were conducted in accordance with the guidelines for the use and care of laboratory animals within the Helmholtz Zentrum München (Germany). Experienced laboratory personnel sacrificed the guinea pigs painlessly by cervical dislocation, and then immediately<sup>42</sup> excised and fixed the heart within the LH apparatus. Hearts were retrograde perfused at constant pressure (800 mmHg) with Krebs–Henseleit buffer (KHB) of the following composition (in mM): 115 NaCl, 5.9 KCl, 1.2 CaCl<sub>2</sub>, 1.2 MgSO<sub>4</sub>, 25 NaHCO<sub>3</sub>, 11.1 D(+)-glucose, 1% bovine serum albumin (BSA). Oxygenation was performed by bubbling carbogen (95% O<sub>2</sub>, 5% CO<sub>2</sub>) through the solution. The pH was set to 7.4, and the temperature was kept at 37.5 °C.

**Electrocardiography, Perfusion Rate, and Heart Rate Measurement.** A scheme of an ECG corresponding to the heart parts is shown in Figure 9. The normal depolarization in the heart begins at the sinus node (SN) near the top of the atrium. In the ECG the P wave represents the wave of depolarization that spreads from the SN throughout the atria. The following isoelectric period represents the time in which the impulse is relayed within the atrioventricular node and the bundle of His to the ventricles. The QRS

complex represents the ventricular depolarization. The isoelectric period (ST segment) following the QRS is the time at which the entire ventricle is depolarized. The ST segment is important in the diagnosis of ventricular ischemia or hypoxia because under those conditions, the ST segment can become either depressed or elevated. The T wave shows the ventricular repolarization and is longer in duration than the depolarization.

All ECG signals were recorded with an EGM Einthoven, Goldberger Module, type 701; the perfusate pressure with a TMA transducer, type 705/1 (Hugo Sachs, D-79232 March-Hugstetten, Germany). In addition, the perfusion rate was determined using an optical drop counter. All signals were digitized with Powerlab 8/30, recorded, and analyzed with the Powerlab System (ADInstruments, D-74937 Spechbach, Germany). The heart rate was calculated from digitized ECGs based on intervals between the R waves. To exclude the effect of extra beats on the heart rate, only R waves in a similar time distance were used and extra beats were excluded using the postevent sleep function of the program.

The heart preparation itself has no influence on the heart function and the ECG response during the experiments. The ECG derived from an animal is the same as from the isolated heart. Using a guinea pig heart the wave shape of the ECG is similar to the human ECG, however the human heart rate is lower by about 66% (see Figure 10). ECGs of other rodents have only a very short ST segment, which is important to detect changes in electrophysiological properties including impulse formation, propagation, and repolarization. Other parameters of the ECG are different from human ECG too (Table 1).

**Experimental Time Protocol.** The whole time protocol was as follows. Isolated guinea pig hearts were perfused for 1 h with KHB (vessel A) to remove blood residues or other contaminations acquired during preparation. However the principal reason is that the heart can restore intracellular energy stores. During heart preparation it is not perfused for a brief period. This leads to a depletion of creatine phosphate and ATP and results in a diminished free-energy of hydrolysis of ATP, activates glycolysis, and causes the accumulation of intracellular lactic acid and the loss of cellular potassium. Because of the disruption of the normal cellular energetic process and the accumulation of these metabolites of ischemia it is important to perfuse the preparation for a duration of time sufficient to wash-out the extracellular compartment and restore cellular energy levels.

The perfusion solution was abolished. Afterward the heart was perfused with KHB from vessel B and the solution was recirculated for 1 h. During this time heart rate reached a steady state level. Then the respective ENPs were added to the perfusion solution. After 1 h the particle concentration was doubled by adding again an adequate amount of ENPs. In control experiments, hearts were subsequently perfused with KHB

without ENPs. ECG, temperature, and perfusion rate were recorded during the entire experiment.

**Catecholamine Determination.** The catecholamine concentration in the perfusion solution was determined by HPLC with coulometric detection according to the published procedure of Smedes *et al.*<sup>43</sup> Determinations were performed by LSM (Labor für Stressmonitoring, Göttingen, Germany).

In brief, 400  $\mu$ L of the acidified liquid perfusion sample was neutralized with 25  $\mu$ L of 2 M NaOH, and 10  $\mu$ L of internal standard DHBA (dihydroxybenzylamine) was added. In a first step the catecholamines bound to diphenylborate with the diol group in an alkaline medium (2 M  $\text{NH}_4\text{OH}/\text{NH}_4\text{Cl}$  buffer, pH 8.6). This catecholamine–diphenylborate complex could be quantitatively extracted into 1.2 mL of a mixture of (*n*-heptane/*n*-octanol, v/v 99:1) by an ion-pair formation with tetraoctylammonium bromide. In a second step, the ion-pair complex was decomposed by acidification with 100 mM acetic acid. The catecholamines could be reextracted and concentrated from 1 mL of the organic extract into 50  $\mu$ L of acetic acid. A 25  $\mu$ L portion of it was injected into the HPLC system. With this extraction procedure the recovery of the catecholamines noradrenaline, adrenaline, and dopamine was higher than 95%.

Chromatographic separation was achieved on a RP C 18 column (150  $\times$  3 mm), packed with 3- $\mu$ m Nucleosil (Macherey & Nagel, Germany), at 35 °C. The citrate-phosphate buffer (pH 4.9; 50 mM) contained 0.27 mM EDTA, 2.5 mM octanesulfonic acid, and 8% (v/v) methanol. The oxidation potential of the electrochemical detector was set to +550 mV. The fully automated HPLC system and the software Chromeleon (Vers. 6.20) was purchased from Dionex Corp. (Idstein, Germany). All chemicals used were of analytical purity. Reproducibility was monitored by the analysis of human plasma control samples (Chromsystems, München, Germany).

**Visualization of Intracellular Free Calcium.** To study whether calcium is involved in catecholamine release from neurons, which are stimulated by ENP, we used neuronal cells (Neuro2A, mouse neuroblastoma, no. ACC 148, DSMZ, Braunschweig, Germany). Fura-2 was used as ratiometric fluorescent dye (Invitrogen, Darmstadt, Germany). Some Fura-2 loaded cells were placed in a temperature controlled observation chamber (1 mL volume) on the stage of a Zeiss Axiovert 100 inverted fluorescence microscope (Zeiss, Göttingen, Germany) and overflowed with KHB containing 1% BSA. By using miniature 2-way valves it was possible to switch rapidly between buffer solution and the nanoparticle-containing solution. The microscope was equipped with a dichroic mirror 400 DCLP and an emitter band-pass 510/40 (AHF Analysentechnik, Tübingen, Germany). A TILL-system and TILLvisiON software (TILL Photonics, Gräfelfing, Germany) was used for excitation (340 and 380 nm), data acquisition, and data calculation. For 2D determination of intracellular free calcium distribution we used a CCD observation. As a measure for intracellular free calcium, the ratio of emission intensities at 340 and 380 nm excitation was determined. With this it was possible to get a reference value and the time course of the effect of ENPs on the calcium homeostasis over a longer time period. Each cell served as its own control.

**ENP Suspensions.** An appropriate amount of ENP samples (see Table 2)  $\text{TiO}_2$ ,  $\text{SiO}_2$ , flame soot Printex P90, spark discharge generated soot, flame derived  $\text{SiO}_2$  (Aerosil), and polystyrene lattices was suspended in 5 mL of KHB containing 1% BSA to reduce particle agglomeration.

The particle suspension was sonicated twice for 1 min using an ultrasonic lance to deagglomerate. The suspension was sequentially filtered through membrane filters of 220 and 100 nm pore size (Millipore MillexGP, Millipore MillexVV) to eliminate agglomerates larger 100 nm. The particle size was determined *in situ* by DLS (dynamic light scattering) using a Malvern HPPS particle sizer (HPPS, Malvern, Herrenberg, Germany) (Figure 11a). We controlled the particle suspension for a few hours for agglomeration and could prove that there was no agglomeration during 6 h (see Figure 11b).

The used membrane filter retains most of the UFP material. Therefore we developed a method to determinate the amount of particles by creating calibration curves using certified monodisperse polystyrene lattices (PSL) of defined diameter (Duke Scientific Corporation, 2463 Faber Place, Palo Alto, California).

A stock solution of UFP was prepared as described above. An aliquot was taken, the absorption coefficient (at a wavelength of 380 nm) was measured, and the size distribution was determined by the particle sizer. Next 40 nm PSL particles were added until the same light backscattering intensity was obtained. In the Rayleigh area a linear dependence consists between the logarithm of the intensity of the back scattered light and the logarithm of the particle size. Using this linearity we calculated the amount of ENPs by the known added amount of PSL which reflected the same light intensity.<sup>19</sup> The same procedure was done for other dilutions. Each measurement was repeated three times and the mean value was calculated. This procedure was done with three different stock solutions. With those values a correlation was obtained between absorption coefficient and particle number concentration. The calibration curve for Printex 90 particles is shown in Figure 12. For each ENP a calibration curve was established. Using the calibration curve it is only necessary to determine the absorption coefficient of the particle suspension after sonication and filtration and to dilute it appropriately.

**Statistical Analysis.** The heart rate was described by a linear mixed regression model for repeated measurements. On the basis of this model, differences between various exposures and control were tested by *F*-tests for the corresponding contrasts. *P*-values less than 0.05 were stated as statistically significant. All calculations were performed by the software package SAS V9.1 (Cary, NC).

**Acknowledgment.** The technical assistance of M. Ellendorff and H. Ferron is gratefully acknowledged. We thank H. Schulz and K. Wittmaack for valuable discussions and critical comments on the manuscript.

## REFERENCES AND NOTES

- Schwerdt, A.; Zintchenko, A.; Conica, M.; Roesen, N.; Fisher, K.; Lindner, L. H.; Issels, R.; Wagner, E.; Ogris, M. Hyperthermia-Induced Targeting of Thermosensitive Gene Carriers to Tumors. *Hum. Gene Ther.* **2008**, *19*, 1283–1292.
- Klotz, S.; Peters, A.; Aalto, A.; Bellander, T.; Berglind, N.; D'ippoliti, D.; Elosua, R.; Hörmann, A.; Kulmala, M.; Lanki, T.; *et al.* Ambient Air Pollution Is Associated with Increased Risk of Hospital Cardiac Readmissions of Myocardial Infarction Survivors in Five European Cities. *Circulation* **2005**, *112*, 3073–3079.
- Schulz, H.; Harder, V.; Ibaldo-Mulli, A.; Khandoga, A.; Koenig, W.; Krombach, F.; Radvkewicz, R.; Stampfl, A.; Thorand, B.; Peters, A. Cardiovascular Effects of Fine and Ultrafine Particles. *J. Aerosol Med.* **2005**, *8*, 1–22.
- Laden, F.; Neas, L. M.; Dockery, D. W.; Schwartz, J. Association of Fine Particulate Matter from Different Sources with Daily Mortality in Six U.S. Cities. *Environ. Health Perspect.* **2000**, *108*, 941–947.
- Brunekreef, B.; Holgate, S. T. Air Pollution and Health. *Lancet* **2002**, *360*, 1233–1242.
- Pope, C. A., III; Hill, R. W.; Villegas, G. M. Particulate Air Pollution and Daily Mortality on Utah's Wasatch Front. *Environ. Health Perspect.* **1999**, *107*, 567–573.
- Yang, Z.; Liu, Z. W.; Allaker, R. P.; Reip, P.; Oxford, J.; Ahmad, Z.; Ren, G. A Review of Nanoparticle Functionality and Toxicity on the Central Nervous System. *J. R. Soc. Interface*, published online, June 2, 2010, DOI: 10.1098/rsif.2010.0158.focus.
- Stoeger, T.; Reinhard, C.; Takanaka, S.; Schroepel, A.; Karg, E.; Ritter, B.; Heyder, J.; Schulz, H. Instillation of Six Different Ultrafine Carbon Particles Indicates a Surface Area Threshold Dose for Acute Lung Inflammation in Mice. *Environ. Health Perspect.* **2006**, *114*, 328–333.
- Monteiro-Riviere, N. A.; Inman, A.; Riviere, J. E. Skin Toxicity of Jet Fuels: Ultrastructural Studies and the Effects of Substance P. *Toxicol. Appl. Pharmacol.* **2004**, *195*, 339–347.
- Lademann, J.; Weigmann, H.; Richtmeyer, C.; Barthelmes, H.; Schäfer, H.; Müller, G.; Sterry, W. Penetration of Titanium Dioxide Microparticles in a Sunscreen Formulation Into the Horny Layer and the Follicular Orifice. *Skin Pharmacol Appl Skin Physiol.* **1999**, *12*, 247–256.



11. Ambrosi, A.; Airo, F.; Merkoz, A. Enhanced Gold Nanoparticle Based ELISA for a Breast Cancer Biomarker. *Anal. Chem.* **2010**, *82*, 1151–1156.
12. Hampel, M. Development of Human 3D *in Vitro* Test Systems for the Risk Assessment of Nanomaterials. PhD Thesis, University Stuttgart, Institute of Interfacial Technology, 2009.
13. Shimada, A.; Kawamura, N.; Okajima, M.; Kaewamatawong, T.; Inoue, H.; Morita, T. Translocation Pathway of the Intracheally Instilled Ultrafine Particles from Lung into Blood Circulation in the Mouse. *Toxicol. Pathol.* **2006**, *34*, 949–957.
14. Geiser, M.; Rothen-Rutishauser, B.; Knapp, N.; Schürch, S.; Kreyling, W.; Schulz, H.; Semmler, M.; Im Hof, V.; Heyder, J.; Gehr, P. Ultrafine Particles Cross Cellular Membranes by Nonphagocytic Mechanisms in Lungs and in Cultured Cells. *Environ. Health Perspect.* **2005**, *113*, 1555–1560.
15. Dhein, S. The Langendorff Heart. In *Practical Methods in Cardiovascular Research*; Springer: Berlin, 2005; pp 155–172.
16. Hearse, D.; Sutherland, F. Experimental Models for the Study of Cardiovascular Function and Disease. *Pharmacol. Res.* **2000**, *41*, 597–603.
17. Bagate, K.; Meiring, J. J.; Gerlofs-Nijland, M. E.; Cassee, F. R.; Wiegand, H.; Osornio-Vargas, A.; Borm, P. J. Ambient Particulate Matter Affects Cardiac Recovery in a Langendorff Ischemia Model. *Inhal. Toxicol.* **2006**, *18*, 633–643.
18. Wold, L. E.; Simkhovich, B. Z.; Kleinman, M. T.; Nordlie, M. A.; Dow, J. S.; Sioutas, C.; Kloner, R. A. *In Vivo* and *In Vitro* Models To Test the Hypothesis of Particle-Induced Effects on Cardiac Function and Arrhythmias. *Cardiovasc. Toxicol.* **2006**, *6*, 69–78.
19. Radykewicz, R. Effects of Ultrafine Modelparticle on Isolated Langendorff Hearts of Guinea Pigs. Ph.D. Thesis, Technical University Munich, Institute of Hydrochemistry, 2007.
20. Rodgers, R. L.; McNeill, J. H. Effect of Reserpine Pretreatment on Guinea Pig Ventricular Performance and Responsiveness to Inotropic Agents. *J. Pharmacol. Exp. Ther.* **1982**, *221*, 721–730.
21. Cairoli, V. J.; Reilly, J. F.; Roberts, J. Effect of Reserpine Pretreatment on the Response of Isolated Papillary Muscle to Ephedrine. *Br. J. Pharmacol. Chemother.* **1962**, *18*, 588–594.
22. Minami, M.; Endo, T.; Hamaue, N.; Hirafuji, M.; Mori, Y.; Hayashi, H.; Sagai, M.; Suzuki, A. K. Electrocardiographic Changes Induced by Diesel Exhaust Particles (DEP) in Guinea Pigs. *Res. Commun. Mol. Pathol. Pharm.* **1999**, *1–2*, 67–76.
23. Crüts, B.; van Etten, L.; Törnqvist, H.; Blomberg, A.; Sandström, T.; Mills, N. L.; Borm, P. J. Exposure to Diesel Exhaust Induces Changes in EEG in Human Volunteers. *Part. Fibre Toxicol.* **2008**, *5*, 4.
24. Zareba, W. Z.; Couderc, J. P.; Oberdörster, G.; Chalupa, D.; Cox, C.; Huang, L.; Peters, A.; Utell, M. J.; Frampton, M. W. ECG Parameters and Exposure to Carbon Ultrafine Particles in Young Healthy Subjects. *Inhalation Toxicol.* **2009**, *21*, 223–233.
25. Hinojosa-Laborde, C.; Lange, D. L. Endothelin Regulation of Adrenal Function. *Clin. Exp. Pharmacol. Physiol.* **1999**, *26*, 995–999.
26. Isaka, M.; Kudo, A.; Imamura, M.; Kawakami, H.; Yasuda, K. Endothelin Receptors, Localized in Sympathetic Nerve Terminals of the Heart, Modulate Norepinephrine Release and Reperfusion Arrhythmias. *Basic Res. Cardiol.* **2007**, *102*, 154–162.
27. Braeuner, E. V.; Forchhammer, L.; Moeller, P.; Simonsen, J.; Glasius, M.; Wahlin, P.; Raaschou-Nielsen, O.; Loft, S. Exposure to Ultrafine Particles from Ambient Air and Oxidative Stress-Induced DNA Damage. *Environ. Health Perspect.* **2007**, *115*, 1177–1182.
28. Risom, L.; Moeller, P.; Loft, S. Oxidative Stress-Induced DNA Damage by Particulate Air Pollution. *Mutat. Res.* **2005**, *592*, 119–137.
29. Ning, L. Ultrafine Particulate Pollutants Induce Oxidative Stress and Mitochondrial Damage. *Environ. Health Perspect.* **2003**, *111*, 455–460.
30. Beck-Speier, I.; Dayal, N.; Karg, E.; Maier, K. L.; Schuhmann, G.; Schulz, H.; Semmler, M.; Takenaka, S.; Stettmeier, K.; Bors, W.; et al. Oxidative Stress and Lipid Mediators Induced in Alveolar Macrophages by Ultrafine Particles. *Free Radic. Biol. Med.* **2005**, *38*, 1080–1092.
31. Kang, J. L.; Moon, C.; Lee, H. S.; Lee, H. W.; Park, E. M.; Kim, H. S.; Castranova, V. Comparison of the Biological Activity Between Ultrafine and Fine Titanium Dioxide Particles in RAW 264.7 Cells Associated with Oxidative Stress. *J. Toxicol. Environ. Health A.* **2008**, *71*, 478–485.
32. Donaldson, K.; Stone, V.; Borm, P. J.; Jimenez, L. A.; Gilmour, P. S.; Schins, R. P.; Knaapen, A. M.; Rahman, I.; Faux, S. P.; Brown, D. M.; et al. Oxidative Stress and Calcium Signalling in the Adverse Effect of Environmental Particles (PM10). *Free Radic. Biol. Med.* **2003**, *34*, 1369–1382.
33. Nel, A. E.; Diaz-Sanchez, D.; Li, N. The Role of Particulate Pollutants in Pulmonary Inflammation and Asthma: Evidence for the Involvement of Organic Chemicals and Oxidative Stress. *Cur. Opin. Pulm. Med.* **2001**, *7*, 20–26.
34. Laurindo, F. R. M.; Pedro, M.; Barbeiro, H. V.; Pileggi, F.; Carvalho, M. H. C.; Augusto, O.; da Luz, P. L. Vascular Free Radical Release: *Ex Vivo* and *In Vivo* Evidence for a Flow-Dependent Endothelial Mechanism. *Circ. Res.* **1994**, *74*, 700–709.
35. Dikalov, S.; Griendling, K. K.; Harrison, D. G. Measurement of Reactive Oxygen Species in Cardiovascular Studies. *Hypertension* **2007**, *49*, 1–11.
36. Zweier, J. L.; Kuppusamy, P.; Lutty, G. A. Measurements of Endothelial Cell Free Radical Generation: Evidence for a Central Mechanism of Free Radical Injury in Postischemic Tissues. *Proc. Natl. Acad. Sci. U.S.A.* **1988**, *85*, 4046–4050.
37. De Keulenaer, G. W.; Andries, L. J.; Sys, S. U.; Brutsaert, D. L. Endothelin-Mediated Positive Inotropic Effect Induced by Reactive Oxygen Species in Isolated Cardiac Muscle. *Circ. Res.* **1995**, *76*, 878–884.
38. Devlin, R. B.; Ghio, A. J.; Kehrl, H.; Sanders, G.; Cascio, W. Elderly Humans Exposed to Concentrated Air Pollution Particles Have Decreased Heart Rate Variability. *Eur. Respir. J.* **2003**, *21*, 76–80.
39. Mahapatrat, N. M.; Mahapatrat, M.; Hazra, P. P.; McDonough, P. M.; ÓConnort, D. T.; Mahata, S. K. A Dynamic Pool of Calcium in Catecholamine Storage Vesicles. Exploration in Living Cells by a Novel Vesicles Targeted Chromogranin A-Aequorin Chimeric Photoprotein. *J. Biol. Chem.* **2004**, *279*, 51107–51121.
40. Mahata, S. K.; O'Connor, D. T.; Mahata, M.; Yoo, S. H.; Taupenot, L.; Wu, H.; Gill, B. M.; Parmer, R. J. Novel Autocrine Feedback Control of Catecholamine Release. A Discrete Chromogranin a Fragment is a Noncompetitive Nicotinic Cholinergic Antagonist. *J. Clin. Invest.* **1997**, *100*, 1623–1633.
41. Niessner, R. Nanoparticles Acting as Condensation Nuclei—Link between Atmosphere and Groundwater Quality? In *Nanoparticles in the Water Cycle*; Frimmel, F., Niessner, R., Eds.; Springer: Berlin, 2010; pp 13–21.
42. Sutherland, S. D.; Festing, M. F. M. The Guinea Pig. In *The UFAW Handbook on the Care and Management of Laboratory Animals*; Poole, T., Ed.; UFAW Publications: Essex, England 1987.
43. Smedes, F.; Kraak, J. C.; Poppe, H. Simple and Fast Solvent Extraction System for Selective and Quantitative Isolation of Adrenaline, Noradrenaline and Dopamine from Plasma and Urine. *J. Chromatogr.* **1982**, *231*, 25–39.